Rheological and Chemical Analysis of Reverse Gelation in a Covalently Cross-Linked Diels−Alder Polymer Network

Brian J. Adzima,[†] H. Alan Aguirre,[†] Christopher J. Kloxin,[†] Timothy F. Scott,[†,‡] and Christopher N. Bowman*[,†]

Department of Chemical and Biological Engineering, University of Colorado, Boulder, Colorado 80309-0424

Received August 15, 2008; Revised Manuscript Received October 3, 2008

ABSTRACT: A network polymer, incorporating dynamic and reversible cross-links, was synthesized using the Diels−Alder reaction. Fourier transform infrared (FTIR) spectroscopy was used to characterize the reaction rate and thermodynamic equilibrium over a broad temperature range. Equilibrium conversion of the furan and maleimide varied from 74% at 85 °C to 24% at 155 °C, demonstrating significant depolymerization via the retro-Diels−Alder reaction. The gel point temperature, as determined by rheometry using the Winter−Chambon criterion, was 92 °C, corresponding to a gel-point conversion of 71%, consistent with the Flory−Stockmayer equation. The scaling exponents for the complex moduli, viscosity, and plateau modulus, in the vicinity of the gel-point, were determined and compared with experimental and theoretical literature values. Further, the material exhibited a low frequency relaxation owing to dynamic rearrangement of cross-links by the Diels−Alder and retro-Diels−Alder reactions.

Introduction

Traditionally, thermosets are irreversibly cross-linked polymeric networks possessing essentially infinite molecular weight that cannot be melted, molded, or dissolved.[1] Such materials are durable and find use in a wide array of applications such as adhesives,[2,3] coatings,[4,5] dental materials,[6,7] and composites.[8,9] In contrast, the incorporation of reversibly labile functionalities into the polymer backbone enables manipulation of network connectivity and allows behavior analogous to melting, molding, and dissolution through depolymerization to low molecular weight species. This reversion significantly extends the capabilities and utility of these cross-linked materials, at the expense of thermal stability. Furthermore, polymers that contain reversible linkages have been used to create stimulus responsive polymers that display novel properties such as shape memory,[10,11] crack healing,[12,13] and stress relief.[14]

In principle, most polymerizations are reversible; however, realizing depolymerization often leads to complete and irreversible degradation of the polymer network. Certain polymers, including those created by radical and ionic polymerization, often depolymerize when heated above a ceiling temperature. Ceiling temperatures are typically quite high and, at such temperatures, irreversible degradation of other molecular structures generally occurs; however, a few polymers, including poly(α-methyl styrene) and poly(isobutene), display more moderate ceiling temperatures (61 and 50 °C, respectively).[15] In condensation polymerizations, condensate removal favors the forward reaction, thus the retro-reaction is only achieved when the condensate is present in significant quantities. Consequently, polymers such as polyacrylhydrazones undergo dynamic network rearrangement, but do not revert to monomer,[16] and exotic approaches are required to create systems that undergo a sol−gel transition, but do not exhibit dynamic network rearrangement in the gel state.[17]

The Diels−Alder (DA) reaction, a [4 + 2] cycloaddition between a diene (e.g., furan) and dieneophile (e.g., maleimide), is thermally reversible via the retro-Diels−Alder (rDA) reaction (Scheme 1).[18] The DA reaction is attractive as a reversible linkage as the rDA reaction occurs at moderate temperatures and does not liberate a small molecule. The subject of more than 17 000 papers, the DA reaction is well studied,[19] but its use in polymer chemistry is comparatively limited. Nevertheless, a variety of macromolecular structures have been synthesized utilizing the DA reaction of maleimides and furans, including linear polymers,[20] networks,[12,13,21,22] hydrogels,[23] and dendrimers.[24] Moreover, DA adducts have been incorporated into monomers bearing other polymerizable functionalities, allowing DA/rDA reactions to be exploited in materials polymerized via common mechanisms such as the reaction between epoxy and amine functionalities,[25] and free-radical (meth)acrylate polymerizations.[26,27]

Network reversibility owing to the rDA reaction has been demonstrated through solubility studies;[21,25,28] however, the temperature dependence of the equilibrium constant, and therefore conversion, in these networks remains relatively unexplored. Typically, polymers above their glass transition temperature have sufficient molecular mobility to reach thermodynamic equilibrium when sufficient time is allowed for completion of the reaction. Accordingly, in polymers formed by the DA reaction, the final conversion is a function of temperature, as demonstrated in linear polymers cross-linked by the DA reaction.[29]

The molecular weight evolution during a step-growth polymerization, such as a DA polymerization, proceeds geometrically and is accompanied by an exponential increase in viscosity. Moreover, for systems capable of cross-linking, the material undergoes gelation, a critical point that occurs when a single macromolecule first spans the sample, and the material transitions from a liquid sol to a solid gel. The creation of a macromolecular gel is accompanied by a divergence in the viscosity and an emergence of an elastic modulus. Typically, as the reaction proceeds, the elastic modulus increases until complete conversion is achieved or the material vitrifies. The mechanical properties of all polymeric materials vary with temperature as they pass through transitions such as crystallization, glass transition, or other molecular relaxations. Unlike conventional, nonreversible networks, the cross-link density of polymers containing DA adducts is dependent on the temperature, leading to the establishment of a gel-point temperature.

* Corresponding author. E-mail: christopher.bowman@colorado.edu.
[†] Department of Chemical and Biological Engineering, University of Colorado.
[‡] Current address: Center for Bioengineering, Department of Mechanical Engineering, University of Colorado, Boulder, Colorado 80309-0427.

10.1021/ma801863d CCC: $40.75
Published on Web 11/04/2008

Scheme 1. Diels-Alder/Retro-Diels-Alder Reaction between a Furan and Maleimide[a]

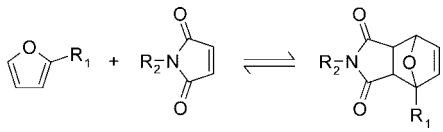

[a] Polymer networks are formed when the Diels−Alder pathway is utilized in monomers with multiple reactive functionalities.

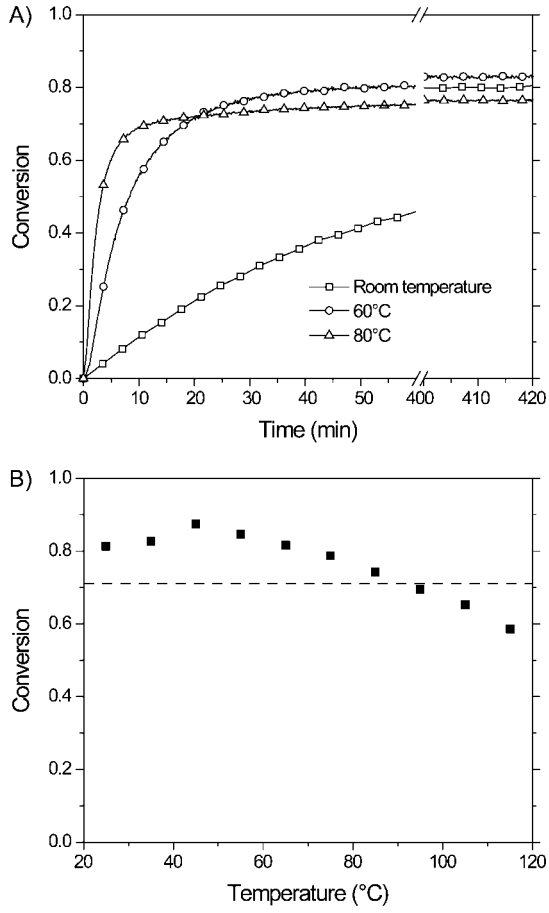

Figure 1. (A) Fractional furan conversion during isothermal polymerizations of 1:1 stoichiometric mixtures of PPTF and DPBM, at various temperatures. (B) Ultimate furan conversion after PPTF-DPBM polymerization. The dashed line represents the gel-point conversion predicted by the Flory−Stockmayer equation, where $f_M = 2$ and $f_F = 3$ (i.e., bismaleimide and trifuran). Maleimide conversions are identical and not plotted for clarity.

The gel-point conversion for the step-growth polymerization between maleimide and furan monomers is well-predicted by the Flory−Stockmayer equation

$$p_g = \frac{1}{\sqrt{r(1-f_M)(1-f_F)}} \quad (1)$$

where p_g is the gel-point conversion, r is the stoichiometric ratio, and f_M and f_F are the degree of functionality for the maleimide and furan monomers, respectively.[30,31] The gel-point conversion is shifted by changing either the monomer functionality or the stoichiometric ratio and determined experimentally using rheometry to compare with the predicted value. Observation of a material's complex response to an oscillatory shear stress allows application of the Winter−Chambon criterion,

$$G'(\omega) \sim G''(\omega) \sim \omega^u \quad (2)$$

which states that the real and imaginary moduli follow identical power law frequency scaling at the gel-point, for $\omega < 1/\tau_0$ where

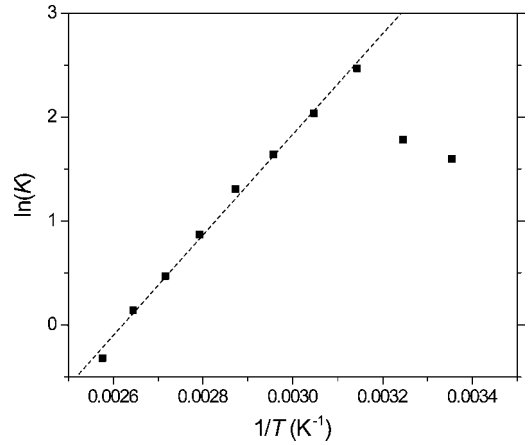

Figure 2. Plot of the natural logarithm of the equilibrium constant (in M^{-1}) versus reciprocal temperature, allows determination of the heat and entropy of reaction through the van't Hoff equation. The fit excludes the data at low temperature where vitrification is evident, preventing the DA reaction equilibrium from being achieved.

τ_0 is the characteristic relaxation time of the smallest molecular species.[32] The gel-point conversion for an irreversible polymerization is typically determined by quenching the reaction, leading to a trial-and-error process. Nevertheless, several researchers have performed accurate mechanical measurements near the gel-point, validating the Winter−Chambon criterion in a rheometer.[33−35] Others have utilized off-stoichiometric monomer ratios so that the gel-point is achieved near the final conversion.[36] Chiou et al. monitored the polymerization of thiol-ene resins using rheometry and inferred the conversion at the gel-point by IR spectroscopy.[37] In contrast, DA-based networks display inherent coupling of conversion and temperature, thereby allowing fine and reversible control of the conversion near the gel-point, all within a single sample.

Here, the reversible reaction between furan and maleimide functionalities is exploited to examine the complex interplay between the Diels−Alder equilibrium, kinetic limitations associated with the mobility in the cross-linked network, the glass transition, and the sol−gel transition using IR spectroscopy and rheometry over a broad temperature range. The mechanical properties of the material are also examined using rheometry as a function of temperature, and therefore conversion, which facilitates the examination of several theoretical descriptions of the gelation process.

Experimental Section

Materials. Pentaerythritol propoxylate triacrylate (PPTA), 1,1′-(methylenedi-4,1-phenylene) bismaleimide (DPBM), furfuryl mercaptan, triethyl amine, and dichloromethane were obtained from Sigma-Aldrich and used without further preparation.

Synthesis of Pentaerythritol Propoxylate Tris(3-(furfurylthiol)-propionate) (PPTF). To a mixture of 10.0 g (0.019 mol) of PPTA and 7.1 g (0.063 mol) of furfuryl mercaptan, a catalytic amount of triethyl amine was added, heated to 40 °C, and allowed to react for 24 h while stirring. The triethylamine and residual furfuryl mercaptan were removed under vacuum (0.2 mmHg) at 45 °C. Absence of peaks in the ^{1}H NMR spectrum of the product due to residual acrylate (6.35, 6.06, and 5.82 ppm) or thiol (1.91 ppm) confirmed complete reaction and subsequent purification of PPTF.

Polymer Synthesis. Polymer samples were prepared by combining PPTF and DPBM at a 1:1 furan to maleimide ratio (Scheme 2). The material was briefly heated (less than 5 min) to ∼155 °C to melt the DPBM, and mixed until homogeneous. Upon cooling, a glassy yellow solid, insoluble in common organic solvents, was formed. The solid material visibly reverted to a liquid upon heating to ∼110 °C.

Scheme 2. Monomers Used for Copolymerization: (A) DPBM, and (B) PPTF, Where $n \sim 1$

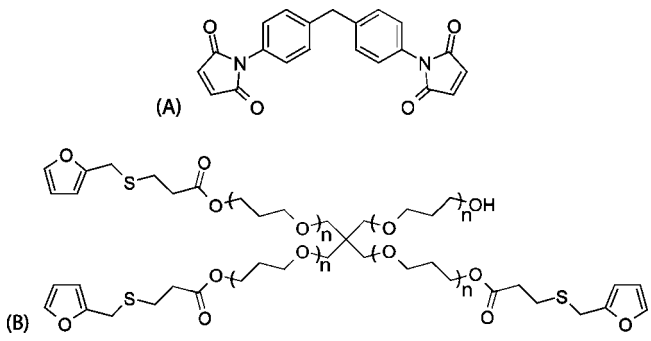

FTIR Spectroscopy. Spectroscopic studies were performed with a Nicolet Magna 750 series II Fourier-transform infrared (FTIR) spectrometer equipped with a MCT detector and a horizontal transmission temperature-controlled stage (accurate to 0.1 °C). Samples for IR spectroscopy were produced by casting a thin film of a freshly prepared solution of PPTF and DPBM in dichloromethane (at a 1:1 furan to maleimide functional group stoichiometric ratio) onto a NaCl crystal and rapidly evaporating the solvent under vacuum. Typically, less than three minutes elapsed between mixing and the initial spectra collection. Reaction during the sample preparation was assumed to be negligible as the DA reaction between furan and maleimide proceeds slowly at ambient temperature. The number of scans per spectrum (between 16 and 512) was adjusted based on the reaction rate. Conversion of the furan and maleimide functionalities was evaluated by monitoring the evolution of the furan peak area, centered at 1010 cm^{-1}, and the maleimide peak area, centered at 690 cm^{-1}.[38,39]

Rheometry. Rheological measurements were performed using an ARES rheometer (TA Instruments), configured with a parallel-plate geometry. The lower fixture incorporated a Peltier plate, providing temperature control, while the upper fixture was equipped with a poly(*p*-phenylene sulfide) (PPS) plate to minimize the temperature gradient across the sample. The polymeric material was heated on the Peltier plate at 115 °C, liquefying the material and enabling intimate contact with both plates. Above and below the gel-point temperature, strain sweeps were conducted from 0.1 to 10 rad/s to verify the material was in the linear viscoelastic regime. Viscosity experiments were conducted over a strain rate ramp from 1.0 to 500 1/s to verify that the material was strain rate independent.

Results and Discussion

FTIR Spectroscopy. Furan conversion (as determined by FTIR spectroscopy) versus time for PPTF-DPBM copolymerizations at several temperatures is shown in Figure 1A. FTIR spectroscopy enables facile determination of both furan and maleimide conversion independently and simultaneously; however, as the functionalities are consumed at equal rates in the DA reaction, for clarity, maleimide conversions are not shown. Whereas the polymerization reaction rate increases monotonically with cure temperature, the ultimate conversion is not monotonically dependent on the temperature. As the polymerization proceeds, there is an increase in the cross-linking density and the glass transition temperature (T_g); however, once the T_g of the polymerizing material equals or exceeds the temperature (T_{cure}), mobility limitations become significant and thus the polymerization rate is severely reduced, i.e., the network vitrifies. Typically, higher cure temperatures result in greater conversions until T_{cure} exceeds the ultimate attainable T_g at full conversion.[40] The increased maximum conversion when the polymerization temperature is raised from ambient to 60 °C (see Figure 1A) is attributed to a delay in the onset of vitrification at the higher temperature. While it might be expected that vitrification should be further delayed at 80 °C (Figure 1A), a decrease in the maximum conversion is observed. As the polymerization temperature is increased above approximately 45 °C, the reaction transitions from kinetic control (a consequence of vitrification) to thermodynamic control associated with the attainment of the equilibrium reaction extent as dictated by the thermodynamics of the DA reaction. This transition can be inferred from Figure 1B where, below 45 °C, vitrification limits the attainable conversion; whereas, above 45 °C, the DA reaction is at or near thermodynamic equilibrium.

Figure 1B illustrates that, above 45 °C, as the temperature is raised, the equilibrium is increasingly driven from the DA adduct to the reactants, via the rDA reaction. The gel-point conversion, as predicted by the Flory−Stockmayer equation, eq 1, is 0.707 for bismaleimide−trifuran polymerization; from the conversion data, the gel-point temperature can be estimated to be 92.5 ± 0.5 °C (Figure 1B). Moreover, the temperature range neighboring the gel-point temperature is well within the thermodynamically controlled reaction regime, allowing facile examination of the gel-point without complications associated with vitrification.

The equilibrium conversion is further decreased to 24% at 155 °C; however, an irreversible side reaction becomes apparent at higher temperatures. At long residence times, above 120 °C, the maleimide peak area begins to decrease, while the furan peak area increases. This decrease in the maleimide peak area likely can be attributed to maleimide homopolymerization, initiated at high temperature as demonstrated by Hopewell et al.,[41] which is accompanied by a corresponding increase in furan concentration as the loss of maleimide drives the equilibrium further toward the reactants.

The equilibrium constant for the reaction between a maleimide (M) and a furan (F), producing a DA adduct (A)

$$K = \frac{[A]}{[M][F]} = \frac{p}{c_0(1-p)^2} \tag{3}$$

can be calculated for a stoichiometric mixture of reactants using the conversion, p (see Figure 1B), and the initial concentration of either reactant, c_0. A plot of the natural logarithm of the equilibrium constant versus inverse temperature, Figure 2, allows the heat of reaction ($\Delta H_r°$) and entropy of reaction ($\Delta S_r°$) to be determined from the slope and intercept. The heat and entropy of reaction were found to be −40 ± 1 kJ/mol and −106 ± 3 J/(mol/s), respectively. This calculated heat of reaction is significantly lower than the reported values (ranging from −84 to −104 kJ/mol) given for reactions between substituted furans with maleic anhydride,[42] however, it compares favorably with an estimate of ∼32 kJ/mol for the kinetically favored endo conformation of a furan−maleimide adduct.[43]

The rate of consumption of furan by reaction with the maleimide is written as

$$\frac{d[F]}{dt} = -k_f[F][M] + k_r[A] \tag{4}$$

where k_f and k_r are the forward and reverse rate constants, respectively. For a stoichiometric mixture of furan and maleimide, the reverse rate constants were determined at 25, 45, 60, and 80 °C (see Supporting Information). The pre-exponential factor and activation energy for the retro DA reaction are determined from an Arrhenius plot to be (5.6 ± 0.3) × 10^9 s^{-1} and 88 ± 2 kJ/mol, respectively (see Figure 3). Activation energies of 102 to 114 kJ/mol have been measured for substituted furans and benzoquinones,[44] suggesting that the measured value is reasonable. The Arrhenius parameter determination allows for the adduct half-life to be expressed as a function of temperature,

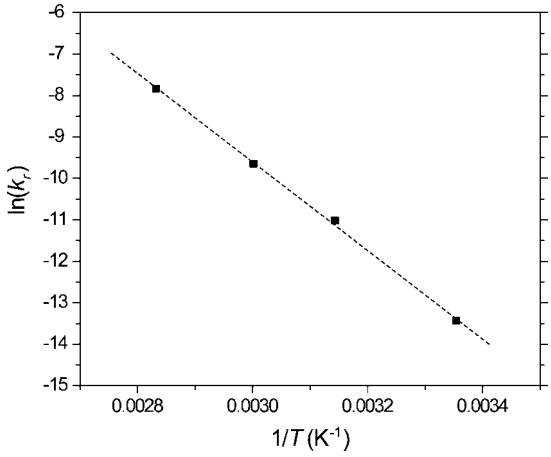

Figure 3. Arrhenius plot of the natural logarithm of the rDA rate constant (in s^{-1}) versus reciprocal temperature. The dashed line represents a fit of the data that allows the pre-exponential factor and activation energy to be determined from the intercept and slope, respectively.

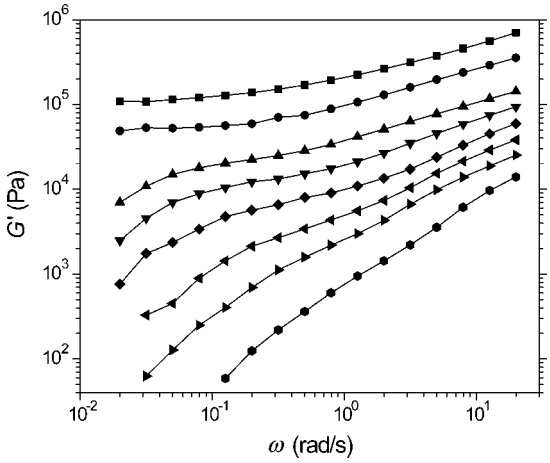

Figure 4. Elastic modulus versus frequency for a PPTF/DPBM network. Frequency sweeps were performed at 75 (■), 80 (●), 85 (▲), 87 (▼), 89 (◆), 91 (triangle pointing left), 93 (triangle pointing right), and 95 °C (⬣).

$$t_{1/2} = \frac{\ln(2)}{k_r} = \frac{\ln(2)}{A_r \exp(-E_a/RT)} \quad (5)$$

The adduct half-life, and thus the half-life of a cross-link, at the gel-point (i.e., 92.5 °C) is calculated to be approximately 600 s, demonstrating the dynamic nature of the DA cross-link. The Arrhenius temperature dependence significantly decreases the reaction rate, and at 66 °C the adduct half-life is approximately 1 order of magnitude longer. At room temperature the adduct half-life is on the order of days.

Rheometry. The application of a small-amplitude sinusoidal deformation to a material yields a complex response, where the modulus is separable into the storage or elastic modulus, G′, and the loss or viscous modulus, *G″*. Here, the behavior of the DA material at low temperatures, or high conversions, is that of a typical cross-linked polymer,[45] demonstrating a constant value for the elastic modulus at low frequency (i.e., a plateau modulus, G_p) as seen in a frequency sweep at 75 °C for the PPTF/DPBM network (Figure 4). As temperature increases, a drop-off in the low-frequency modulus occurs (Figure 4), and a cross-over in the elastic and viscous moduli is observed (Figure 5), demonstrating liquid-like behavior and relaxation at long timescales. Typical chemical gels form irreversible bonds; however, DA cross-links are dynamic,

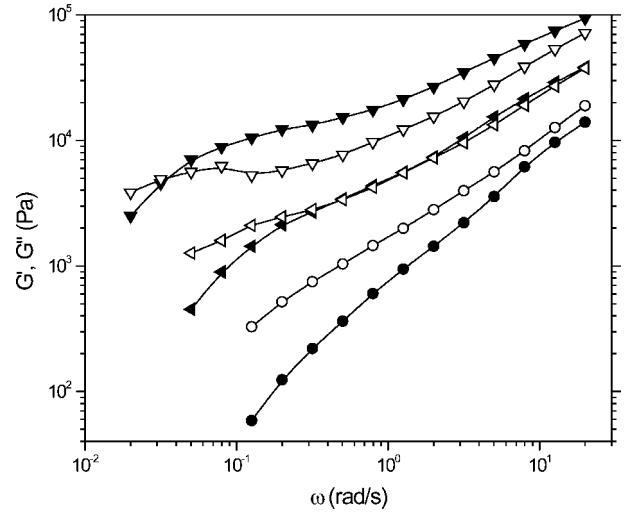

Figure 5. Elastic (filled symbols) and viscous (open symbols) moduli versus frequency at temperatures above (95 °C, ●), near (91 °C, triangle pointing left), and below (87 °C, ▼) the gel-point temperature.

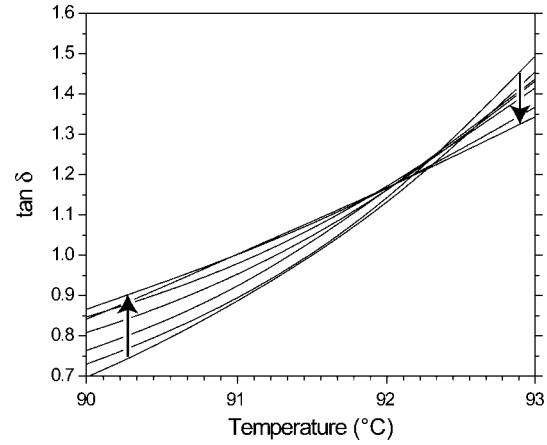

Figure 6. Tan δ for several frequencies between 0.63 and 10 rad/s versus temperature for a single, representative data set, demonstrating frequency independence (i.e., a cross-over) at 92.1 °C. The upper and lower frequency limits are within the valid range of the Winter−Chambon criterion, where $1/\tau_L < 1/\tau_0$. Directions of arrows indicate increasing frequency.

constantly breaking and reforming over timescales dictated by the DA reaction kinetics and mobility restrictions, resulting in continuous network rearrangement on timescales associated with the temperature-dependent kinetics described above for the DA and rDA reactions. This low frequency behavior is analogous to that displayed by physical gels, such as gelatin,[46] which are connected by chain entanglements and other weak associations such as hydrogen bonds or ionic interactions, allowing network relaxation at long timescales. Network rearrangement has the consequence of adding a lower frequency bound to the Winter−Chambon criterion (eq 2), corresponding to the longest relaxation time of the network, τ_L. It should be noted that the relaxation in the DA network, as determined by the G′–G″ cross-over at 87 °C, occurs on, the same order of magnitude, $10^2 - 10^3$ s, as the half-life of the adduct determined from the kinetics.

Several distinguishing mechanical properties of the DA material, readily observed by rheometry, can be used to characterize its sol and gel states (see Figure 5). When the DA material is heated to 95 °C, above the gel-point temperature (i.e., below the gel-point conversion), the viscous modulus is greater than the elastic modulus, characteristic of a liquid-like sol. Conversely, the elastic modulus is greater than the viscous modulus at 87 °C for most of the frequency range, characteristic

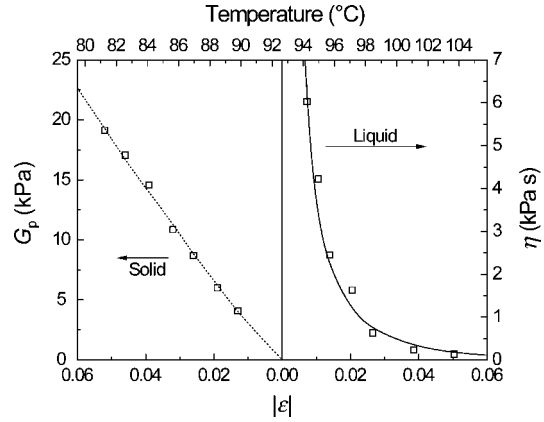

Figure 7. Plateau modulus (left) and the viscosity (right) as a function of the relative distance from the gel point and temperature. The lines indicate the fits of the data to (7) and (8) on the liquid and solid sides, respectively.

of a solid-like gel. At 91 °C, the elastic and viscous moduli exhibit similar frequency scaling at higher frequencies, indicating that the material is near the gel-point as defined by the Winter−Chambon criterion, eq 2; however, unlike typical chemical gels, the moduli exhibit liquid-like scaling at lower frequency owing to network relaxation.

The Winter−Chambon criterion, eq 2, can be re-expressed in terms of the ratio of the viscous to elastic modulus (i.e., tan δ) which, at the gel-point, demonstrates frequency independence. A plot of constant frequency tan δ curves versus temperature (Figure 6) reveals an intersection that precisely marks the gel-point. The gel-point temperature was thus determined from several data sets to be 92.1 ± 0.2 °C, corresponding to a conversion of 70.9 ± 0.5%, in excellent agreement with the gel-point conversion predicted by the Flory−Stockmayer equation, eq 1. Whereas other researchers have demonstrated some extent of reverse polymerization at raised temperatures, to our knowledge, this is the first clear demonstration of a temperature controlled sol−gel transition in cross-linked DA polymers, in the absence of a solvent. For example, high temperature ^{13}C NMR spectroscopy performed on crack-healing DA materials demonstrated reversion to 70% conversion; however, the tetrafuran-trimaleimide system used in that work would require a reversion to 40.1% conversion to achieve reverse gelation, indicating that "softening" and "remendability" was achieved exclusively through network rearrangement rather than liquid flow.[12]

The frequency cross-over in tan δ determines the frequency scaling of the storage and loss moduli, u, through the relationship,[47]

$$\delta = \frac{u\pi}{2} \tag{6}$$

yielding $u = 0.56 \pm 0.02$. As the conversion approaches the gel-point from the sol phase (i.e., the liquid side of Figure 7), the viscosity divergence is described by the power law,

$$\eta \sim |\varepsilon|^{-s} \tag{7}$$

while the emergence of a plateau modulus, beyond the gel-point (i.e., the solid side of Figure 7), is described by the power law,

$$G_p \sim |\varepsilon|^t \tag{8}$$

where ϵ is the relative distance from the gel point

$$\varepsilon \equiv \frac{p - p_{gel}}{p_{gel}} \tag{9}$$

and s and t are characteristic scaling exponents.

Table 1. Experimental and Theoretical Values of Scaling Exponents Associated with Gelation

	u	s	t	ref
mean field	1	0	3	31, 53
electrical−mechanical analogy	0.72	0.75	1.9	50, 53
Rouse model	0.67	1.3	2.6	51
experiment	0.56 ± 0.02	1.4 ± 0.2	1.23 ± 0.03	

The diverging and subsequent emerging nature of the viscosity and modulus, respectively, in the vicinity of the gel-point are shown in Figure 7. A zero shear modulus is not observed in DA networks owing to their long-time relaxation, and is thus supplanted by the corresponding plateau modulus as determined by the inflection point in the elastic modulus. The plateau modulus was normalized by the temperature to eliminate the entropic contribution ($G \sim T$, i.e., via rubber elasticity) and fit to eq 8 (dashed line, Figure 7), yielding $t = 1.23 \pm 0.03$. The viscosity was fit to eq (7) (solid line, Figure 7) and normalized by the activation energy (i.e., $\eta \sim \exp(E_a/RT)|\varepsilon|^{-s}$), yielding $s = 1.4 \pm 0.2$.

The scaling exponents u, s, and t are the foundation for a universal description of gelation. Several theories attempt to predict these exponents, an overview of which is shown in Table 1. Mean field approaches have been used, but are typically successful only at high values of ϵ or when the distances between branch points are large, e.g., vulcanization.[31,48,49] De Gennes' electrical–mechanical analogy establishes an equivalent scaling of the modulus and macroscopic conductivity and, unlike mean field theory, predicts the divergence of the viscosity.[50] The Rouse model describes linear polymers as a series of identical beads and springs, and assumes hydrodynamic interactions are screened at sizes smaller than the monomer level. The Rouse model can be extended to describe networks and has been shown to predict the scaling exponents successfully when the distance between network junctions is small.[51,52]

For the DA material, the frequency scaling of the elastic and viscous moduli at the gel-point, u, is most similar to the Rouse model prediction. For other systems, experimental values have been observed to be in the range of 0.19 to 0.92.[54,55] Deviations of u from the Rouse model prediction have been suggested to occur because of chain overlap,[49,52] and the discrepancy between the measured value and the Rouse model may occur because the molecular weight of the PPTF monomer is sufficient to allow chain overlap. Such behavior would be manifest by a value of u less than that predicated by the Rouse model.

The viscosity scaling exponent s agrees well with both the Rouse model prediction and literature values.[34,56] It should be noted, however, that the error indicated for s only reflects random error and not the systematic error in the gel-point conversion, which can have considerable impact on the scaling determination. As the scaling exponents (i.e., u, s, and t) are interdependent and are related through[49,52,55]

$$t = \frac{su}{1-u} \tag{10}$$

the experimentally determined values for the exponents u and s can be used to calculate the plateau modulus exponent, yielding $t = 1.8 \pm 0.3$. This value is inconsistent with the experimentally determined value for t (see Table 1), which could simply be due to the sensitivity of the exponents to the precise location of the gel-point conversion.

Conclusions

A cross-linked polymer was formed by the DA reaction between furan and maleimide moieties, and the furan conversion was measured using FTIR spectroscopy. Below 45 °C, vitrification limited the ultimate attainable conversion, while above 45 °C, the

final conversion is determined by the thermodynamic equilibrium. At sufficiently elevated temperatures, the equilibrium shift through the retro-DA reaction results in depolymerization and reverse gelation. The gel-point temperature of the material was determined by the Winter−Chambon criteria to be 92.1 ± 0.2 °C, which, in conjunction with spectroscopic data, is consistent with the gel-point predicted by the Flory−Stockmayer equation for trifuran-bismaleimide system. The DA adduct half-life was on the same order of magnitude as the longest relaxation time for the network at 87 °C, further illustrating the dynamic nature of the DA cross-link. The rapid and temperature dependent reversible DA reaction enables facile manipulation of conversion and thus allows the scaling exponents u, s, and t to be determined in the vicinity of the gel-point. These exponents were found to be similar to other values in the literature; however, they were not consistent with values predicted from mean field theory, electrical−mechanical analogy, or the Rouse model.

Networks formed by the Diels−Alder reaction have been proposed for remendability, recyclability, and removability, properties that are not accessible in conventional thermosets. The crack healing ability of these networks can be attributed to the constant breaking and reforming of cross-links, which allows affected areas to form new cross-links. Furthermore, because the reaction is controlled by thermodynamics over a large temperature range, the cross-linking density can be controlled and these materials can be removed and recycled by reversion to low molecular weight species. These results not only demonstrate the utility of the Diels−Alder reaction in polymer science, but they also illustrate the potential of reversibly labile cross-links for the creation of novel materials.

Acknowledgment. The authors acknowledge funding from the Department of Education GAANN Fellowship (B.J.A.); NSF REU (H.A.A.); and the National Institutes of Health NIH Grant DE 10959 (C.J.K., T.F.S., and C.N.B.).

Supporting Information Available: Text giving a detailed solution of the kinetic rate equation, rate constant calculation, and a plot of the fit to data of conversion vs time. This material is available free of charge via the Internet at http://pubs.acs.org.

References and Notes

(1) Billmeyer, R. *Textbook of Polymer Science*; John Wiley and Sons: New York, 1984.
(2) Kloosterboer, J. G. *Adv. Polym. Sci.* **1988**, *84*, 1–61.
(3) Hoyle, C. E.; Lee, T. Y.; Roper, T. *J. Polym. Sci., Part A: Polym. Chem.* **2004**, *42*, 5301–5338.
(4) Oshima, A.; Abe, K.; Kameda, N. Process for producing abrasion-resistant cast article. U.S. Patent 3,978,178, **1976**.
(5) Decker, C. *Macromol. Rapid Commun.* **2002**, *23*, 1067–1093.
(6) Anseth, K. S.; Newman, S. M.; Bowman, C. N. Polymeric dental composites: Properties and reaction behavior of multimethacrylate dental restorations. *Biopolymers Ii* **1995**, *122*, 177–217.
(7) Lu, H.; Stansbury, J. W.; Bowman, C. N. *Dent. Mater.* **2004**, *20*, 979–986.
(8) Urabe, H.; Wakasa, K.; Yamaki, M. *J. Mater. Sci.—Mater. Med.* **1990**, *1*, 163–170.
(9) LeBaron, P. C.; Wang, Z.; Pinnavaia, T. J. *Appl. Clay Sci.* **1999**, *15*, 11–29.
(10) Inoue, K.; Yamashiro, M.; Iji, M. *Kobunshi Ronbunshu* **2005**, *62*, 261–267.
(11) Lendlein, A.; Jiang, H. Y.; Junger, O.; Langer, R. *Nature* **2005**, *434*, 879–882.
(12) Chen, X. X.; Dam, M. A.; Ono, K.; Mal, A.; Shen, H. B.; Nutt, S. R.; Sheran, K.; Wudl, F. *Science* **2002**, *295*, 1698–1702.
(13) Chen, X. X.; Wudl, F.; Mal, A. K.; Shen, H. B.; Nutt, S. R. *Macromolecules* **2003**, *36*, 1802–1807.
(14) Scott, T. F.; Schneider, A. D.; Cook, W. D.; Bowman, C. N. *Science* **2005**, *308*, 1615–1617.
(15) Odian, G., *Principles of Polymerization*. 3rd ed.; John Wiley and Sons, Inc.: New York, 1991.
(16) Ono, T.; Nobori, T.; Lehn, J. M. *Chem. Commun.* **2005**, 1522–1524.
(17) Yurke, B.; Lin, D. C.; Langrana, N. A. Use of DNA nanodevices in modulating the mechanical properties of polyacrylamide gels. *DNA Comput.* **2006**, *3892*, 417–426.
(18) March, J., *Advanced Organic Chemistry: Reactions, Mechanisms, and Structure*; John Wiley and Sons: New York, 1992; p 830.
(19) Fringuelli, F.; Taticchi, A., *The Diels-Alder Reaction*; John Wiley and Sons: New York, 2002.
(20) Gousse, C.; Gandini, A. *Polym. Int.* **1999**, *48*, 723–731.
(21) Canary, S. A.; Stevens, M. P. *J. Polym. Sci., Part A: Polym. Chem.* **1992**, *30*, 1755–1760.
(22) Imai, Y.; Itoh, H.; Naka, K.; Chujo, Y. *Macromolecules* **2000**, *33*, 4343–4346.
(23) Chujo, Y.; Sada, K.; Saegusa, T. *Macromolecules* **1990**, *23*, 2636–2641.
(24) Szalai, M. L.; McGrath, D. V.; Wheeler, D. R.; Zifer, T.; McElhanon, J. R. *Macromolecules* **2007**, *40*, 818–823.
(25) McElhanon, J. R.; Russick, E. M.; Wheeler, D. R.; Loy, D. A.; Aubert, J. H. *J. Appl. Polym. Sci.* **2002**, *85*, 1496–1502.
(26) Heath, W. H.; Palmieri, F.; Adams, J. R.; Long, B. K.; Chute, J.; Holcombe, T. W.; Zieren, S.; Truitt, M. J.; White, J. L.; Willson, C. G. *Macromolecules* **2008**, *41*, 719–726.
(27) Long, B. K.; Keitz, B. K.; Willson, C. G. *J. Mater. Chem.* **2007**, *17*, 3575–3580.
(28) Gousse, C.; Gandini, A.; Hodge, P. *Macromolecules* **1998**, *31*, 314–321.
(29) Chang, B. T. A.; Dubois, D. A.; Ming, F.; Gelles, D. L.; Iyer, S. R.; Mohindra, S.; Tutunjian, P. N.; Wong, P. K.; Wright, W. J. CARIVERSE resin: a thermally reversible network polymer for electronic applications. In *Electronic Components and Technology Conference. 1999 Proceedings. 49th*; **1999**; pp49−55.
(30) Flory, P. J. *J. Am. Chem. Soc.* **1941**, *63*, 3083–3090.
(31) Stockmayer, W. H. *J. Chem. Phys.* **1943**, *11*, 45–55.
(32) Winter, H. H. *Polym. Eng. Sci.* **1987**, *27*, 1698–1702.
(33) Adolf, D.; Martin, J. E.; Wilcoxon, J. P. *Macromolecules* **1990**, *23*, 527–531.
(34) Hodgson, D. F.; Amis, E. J. *J. Non-Cryst. Solids* **1991**, *131*, 913–920.
(35) Lairez, D.; Adam, M.; Emery, J. R.; Durand, D. *Macromolecules* **1992**, *25*, 286–289.
(36) Lairez, D.; Adam, M.; Raspaud, E.; Emery, J. R.; Durand, D. *Prog. Colloid Polym. Sci.* **1992**, *90*, 37–42.
(37) Chiou, B. S.; English, R. J.; Khan, S. A. *Macromolecules* **1996**, *29*, 5368–5374.
(38) Decker, C.; Bianchi, C.; Jonsson, S. *Polymer* **2004**, *45*, 5803–5811.
(39) Tarducci, C.; Badyal, J. P. S.; Brewer, S. A.; Willis, C. *Chem. Commun.* **2005**, 406–408.
(40) Enns, J. B.; Gillham, J. K. *J. Appl. Polym. Sci.* **1983**, *28*, 2567–2591.
(41) Hopewell, J. L.; Hill, D. J. T.; Pomery, P. J. *Polymer* **1998**, *39*, 5601–5607.
(42) Dewar, M. J. S.; Pierini, A. B. *J. Am. Chem. Soc.* **1984**, *106*, 203–208.
(43) Rulisek, L.; Sebek, P.; Havlas, Z.; Hrabal, R.; Capek, P.; Svatos, A. *J. Org. Chem.* **2005**, *70*, 6295–6302.
(44) Jurczak, J.; Kawczynski, A. L.; Kozluk, T. *J. Org. Chem.* **1985**, *50*, 1106–1107.
(45) Ferry, J. D., *Viscoelastic Properties of Polymers*, 3rd ed.; John Wiley and Sons: New York, 1980.
(46) Nijenhuis, K. T. Thermoreversible networks—Viscoelastic properties and structure of gels. *Thermoreversible Networks* **1997**, *130*000.
(47) Michon, C.; Cuvelier, G.; Launay, B. *Rheol. Acta* **1993**, *32*, 94–103.
(48) de Gennes, P. G., *Scaling Concepts in Polymer Physics*; Cornell Univeristy Press: Ithaca, NY, and London, 1979.
(49) Lusignan, C. P.; Mourey, T. H.; Wilson, J. C.; Colby, R. H. *Phys. Rev. E* **1999**, *60*, 5657–5669.
(50) de Gennes, P. G. *J. Phys. Paris* **1976**, *37*, L-1.
(51) Rubenstein, M.; Colby, R. H.; Gillmor, J. R.; Dynamic Scaling for Polymer Gelation. In *Space-Time Organization in Macromolecular Fluids*; Tanaka, F., Doi, M., Ohta, T., Springer-Verlag: Berlin, 1989; Vol. *30*.
(52) Lusignan, C. P.; Mourey, T. H.; Wilson, J. C.; Colby, R. H. *Phys. Rev. E* **1995**, *52*, 6271–6280.
(53) Devreux, F.; Boilot, J. P.; Chaput, F.; Malier, L.; Axelos, M. A. V. *Phys. Rev. E* **1993**, *47*, 2689–2694.
(54) Scanlan, J. C.; Winter, H. H. *Macromolecules* **1991**, *24*, 47–54.
(55) Durand, D.; Delsanti, M.; Adam, M.; Luck, J. M. *Europhys. Lett.* **1987**, *3*, 297–301.
(56) Guo, L.; Colby, R. H.; Lusignan, C. P.; Howe, A. M. *Macromolecules* **2003**, *36*, 10009–10020.

MA801863D